Published in final edited form as:

Biochem J. 2008 August 15; 414(1): 31–41. doi:10.1042/BJ20071240.

Sphingomyelin synthases regulate production of diacylglycerol at the Golgi

Maristella Villani[*,†], **Marimuthu Subathra**[*], **Yeong-Bin Im**[*], **Young Choi**[*], **Paola Signorelli**[‡], **Maurizio Del Poeta**[*,§,‖], and **Chiara Luberto**[*,1]

[*]Department of Biochemistry and Molecular Biology, Medical University of South Carolina, Charleston, SC 29425, U.S.A.

[†]Biochemical Sciences and Molecular Biotechnology, Division of Physiopathology, University of Perugia, Italy

[‡]Laboratory of Biochemistry and Molecular Biology, San Paolo University Hospital, School of Medicine, University of Milan, 20142 Milan, Italy

[§]Microbiology and Immunology, Medical University of South Carolina, Charleston, SC 29425, U.S.A.

[‖]Division of Infectious Diseases, Medical University of South Carolina, Charleston, SC 29425, U.S.A.

Abstract

SMS [SM (sphingomyelin) synthase] is a class of enzymes that produces SM by transferring a phosphocholine moiety on to ceramide. PC (phosphatidylcholine) is believed to be the phosphocholine donor of the reaction with consequent production of DAG (diacylglycerol), an important bioactive lipid. In the present study, by modulating SMS1 and SMS2 expression, the role of these enzymes on the elusive regulation of DAG was investigated. Because we found that modulation of SMS1 or SMS2 did not affect total levels of endogenous DAG in resting cells, whereas they produce DAG *in vitro*, the possibility that SMSs could modulate subcellular pools of DAG, once acute activation of the enzymes is triggered, was investigated. Stimulation of SM synthesis was induced by either treatment with short-chain ceramide analogues or by increasing endogenous ceramide at the plasma membrane, and a fluorescently labelled conventional C1 domain [from PKC (protein kinase C)] enhanced in its DAG binding activity was used to probe subcellular pools of DAG in the cell. With this approach, we found, using confocal microscopy and subcellular fractionation, that modulation of SMS1 and, to a lesser extent, SMS2 affected the formation of DAG at the Golgi apparatus. Similarly, down-regulation of SMS1 and SMS2 reduced the localization of the DAG-binding protein PKD (protein kinase D) to the Golgi. These results provide direct evidence that both enzymes are capable of regulating the formation of DAG in cells, that this pool of DAG is biologically active, and for the first time directly implicate SMS1 and SMS2 as regulators of DAG-binding proteins in the Golgi apparatus.

[1]To whom correspondence should be addressed (luberto@musc.edu).

Keywords

ceramide; diacylglycerol; diacylglycerol-binding domain; Golgi; sphingolipid; sphingomyelin synthase

INTRODUCTION

SMSs [SM (sphingomyelin) synthases] represent a class of enzymes involved in the synthesis of SM, an abundant phospholipid with an important structural role in the integrity of the plasma membrane. PC (phosphatidylcholine) is the proposed donor of the phosphocholine group that SMS transfers on to the primary hydroxy group of ceramide, generating DAG (diacylglycerol) as an additional product of the reaction [1–5]. Therefore it has been suggested that the biological importance of SMSs resides not only in the biosynthesis of SM but also in the regulation, in opposing directions, of the levels of ceramide, a bioactive molecule which often exerts a negative effect on cell proliferation, and DAG, a well-established signalling lipid [6]. Moreover, SMS activity, through the control of the levels of SM and ceramide, could also be involved in the functional modulation of plasma membrane lipid rafts [7,8].

In support of a role for SMS that goes beyond the housekeeping function of SM synthesis, positive regulation of its activity has been reported in association with conditions of enhanced proliferation and transformation, such as hepatic regeneration, astrocytes stimulated with bFGF (basic fibroblast growth factor), SV40 (simian virus 40)-transformed fibroblasts and hepatocellular carcinoma [6,9,10]. On the other hand, caspase-dependent inhibition of SMS activity has been observed upon initiation of apoptosis by TNF (tumour necrosis factor) in Kym-1 rhabdomyosarcoma cells [11] or Fas cross-linking in Jurkat cells [12] that led to the hypothesis that inhibition of SMS could be a regulated process required for the full development of the apoptotic programme.

So far, only a few potential downstream targets for SMS have been identified. In particular, it has been proposed that activation of SM synthesis in response to growth initiation of Madin–Darby canine kidney cells by serum stimulation led to production of DAG which correlated with activation of PKC (protein kinase C) as measured by means of its membrane translocation [13]. Indirect evidence for a role of SMS in the regulation of PKC comes from studies in U937 human monocytic leukaemia cells where the use of a pharmacological inhibitor of SMS, D609, induced a significant accumulation of ceramide and a pronounced decrease in DAG levels, followed by cell death. Pretreatment with the PKC activator PMA or supplementation with a cell-permeable DAG analogue greatly attenuated D609-mediated cytotoxicity, bypassing the effect of SMS inhibition [14]. Additional studies from our group showed that active SM synthesis correlated with nuclear translocation and activation of NF-κB (nuclear factor κB) [15], an important transcription factor often linked to survival pathways and inflammatory responses. Finally, DAG derived from sphingolipid metabolism has been potentially linked to translocation of PKD (protein kinase D) to the Golgi [16].

Mammalian SMSs (namely, SMS1 and SMS2) have only been recently identified molecularly [17,18]. Overall, no significant biochemical differences have been found

between SMS1 and SMS2 [17]. On the other hand, a different cellular localization was shown for the two SMSs when expressed in HeLa human cervical carcinoma cells, where SMS1 localized in the Golgi and SMS2 in Golgi and plasma membrane [17]. This localization pattern is in agreement with earlier biochemical studies using fractionation techniques that reported the bulk of SMS activity in the Golgi and residual activity in other cellular compartments, including plasma membrane [3,19].

Studies conducted in mammalian models have confirmed the ability of both SMSs to regulate the levels of SM and ceramide in cells [7,18,20–23]. On the other hand, no clear evidence for involvement of SMS1 or SMS2 in the regulation of DAG was provided. In fact, in these reports, down-regulation of either SMS did not induce significant changes in either PC or DAG levels.

In the present study, we employed both downregulation through siRNA (short interfering RNA) and up-regulation through overexpression to study the role of SMS1 and SMS2 in the regulation of DAG levels. After validation of the effects of our siRNA sequences and expression system, we show that both SMS1 and SMS2 are capable of regulating DAG formation at the Golgi and, by doing so, that they affect the localization of the DAG-binding protein PKD in this compartment.

EXPERIMENTAL

Materials

DMEM (Dulbecco's modified Eagle's medium) and RPMI 1640 medium, trypsin/EDTA and FBS (fetal bovine serum) were from Gibco/Invitrogen; anti-FLAG monoclonal antibodies were from Sigma and anti-(mouse IgG) was purchased from Santa Cruz Biotechnology; and anti-V5 monoclonal antibodies were purchased from Invitrogen. NBD [*N*-(7-nitrobenz-2-oxa-1,3-diazol-4-yl)]-C_6-ceramide and NBD-C_6-SM were purchased from Molecular Probes. [9,10-^{3}H(n)]Palmitic acid and [*methyl*-^{3}H]choline chloride were purchased from American Radiolabeled Chemicals. All other lipids were purchased from Avanti Polar Lipids (Alabaster, AL, U.S.A.).

Cell culture

HeLa and SV40-transformed WI38 (fibroblast) cells were cultured in high glucose DMEM. The medium was supplemented with 10% FBS and cells were grown at 37°C in a humidified 5% CO_2 incubator.

Down-regulation of SMS1 and SMS2

Down-regulation of SMS1 or SMS2 was achieved with siRNA oligonucleotides targeting *SMS1* (CACACTATGGCCAATCAGCAA) or *SMS2* (AAGGCACCAAAAAGTACCCGG) synthesized by Qiagen, and by using Oligofectamine™ transfection reagent (Invitrogen). The non-specific All Star siRNA sequence (SCR; scrambled siRNA) was used as control (Qiagen). Typically, 0.2–0.23 × 10^6 HeLa cells from an exponentially growing culture not exceeding 20 passages were plated in 10-cm-diameter dishes. After approx. 24 h, cells were transfected with siRNA according to the manufacturer's instructions in a total of 6 ml of

transfection mixture containing siRNA and Oligofectamine™ in Optimem medium. After 6 h of incubation, 6 ml of DMEM containing 20% FBS was added to the plates.

DAG measurements

DAG levels were evaluated using the *Escherichia coli* DGK (diacylglycerol kinase) assay as described in [6].

SMS assay

HeLa cells were collected and homogenized in ice-cold lysis buffer by 20 passages through a 28.5 gauge needle. The lysis buffer contained 25 mM Tris/HCl (pH 7.4), 5 mM EDTA and 1 mM PMSF. Cell lysates were centrifuged at 300 ***g*** for 5 min at 4°C, and the supernatant was used for measuring the enzymatic activity. Protein concentrations were determined using the Bio-Rad assay. The SMS assay was performed using 50 μg of protein. The substrate was prepared as a mixture of 40 μM NBD-C_6-ceramide and 200 μM PC resuspended in 100 mM Tris/HCl (pH 7.4), 50 mM KCl and 1 mM EDTA by sonication and vortexing until clear. For the experiments in which NBD-C_6- or NBD-C_{12}-PC were used, the substrate was prepared as a mixture of 40 μM C_6-ceramide, 100 μM NBD-PC and 100 μM natural PC. The substrate was diluted 1:1 with the proteins resuspended in lysis buffer (final incubation volume of 100 μl), and the incubation was carried out for 30 min in the dark at 30 °C. The reaction was stopped on ice by addition of 3 vol. of chloroform/methanol (1:1, v/v). After vortexing, the phases were clarified by centrifugation at 2400 ***g*** for 5 min. The lower phase was transferred to new tubes, dried down, and lipids were resuspended with 40 μl of chloroform/methanol (2:1, v/v) and separated by TLC in chloroform/ methanol/15 mM $CaCl_2$ (90:52.5:12, by vol.). Fluorescence was measured using a Storm 860 Imaging Analysis System from Amersham Biosciences (U.K.). Results were analysed using ImageQuant software from Amersham Biosciences.

Overexpression of FLAG–SMSs or SMS2–V5

HeLa cells were plated using 0.3×10^6 cells per 10-cm-diameter dish. After 2 days, cells were transfected with 1 μg of pcDNA3.1 containing a FLAG-tagged version of SMS1 or SMS2 at the N-terminus (FLAG–SMS1 or FLAG–SMS2) or SMS2 with V5 tag at the C-terminus by the Effectene® transfection reagent from Qiagen according to the manufacturer's instructions. The constructs were obtained by PCR of full-length cDNA clones purchased from Open Biosystems (Alabama), for FLAG–SMS1 the 5′-primer CAATAAGCTTGCCACCATGGATTACAAGGATGACGACGATAAGAAGGAAGTGGTTTATTGGTCAC and the 3′-primer CACGAATTCTTATGTGTCATTCACCAGCCGGCTG was used; for FLAG–SMS2 the 5′-primer CAATAAGCTTGCCACCATGGATTACAAGGATGACGACGATAAGGATATCATAGAGACAGCAAAAC and 3′-primer CACGAATTCTCAGGTCGATTTCTCATTGTCTTCAC was used; for SMS2-V5 the 5′-primer CAATAAGCTTGCCACCATGGATATCATAGAGACAGCAAAACTTG and the 3′-primer CACGAATTCTCACGTAGAATCGAGACCGAGGAGAGGGTTAGGGATAGGCTTACCGGTCGATTTCTCATTGTCTTCAC was used.

Cellular metabolism of NBD-C_6-ceramide

HeLa cells were plated in 10-cm-diameter dishes at a density of either 0.2×10^6 or at 0.3×10^6 for silencing RNA or overexpression of FLAG–SMS1 and FLAG–SMS2 respectively. After 48 h and 72 h of siRNA treatment or 36 h of overexpression, cells were treated in fresh medium with 5 μM NBD-C_6-ceramide for up to 8 h. Cells were scraped in 2 ml of ice-cold PBS, and each plate was washed with an additional 2 ml of PBS. Cells and washes were combined and centrifuged for 5 min at 1000 ***g*** (4 °C). Lipids were extracted from cell pellets as using the method of Bligh and Dyer [24]. The organic phase was separated into two aliquots of 300 μl for lipid phosphorus determination and 1 ml for lipid analysis. The organic phase for lipid analysis was dried down, and lipids were resuspended with 50 μl of chloroform/methanol (2:1, v/v) and then separated by TLC in chloroform/methanol/15 mM $CaCl_2$ (90:52.5:12, by vol.). Fluorescence was measured using a Storm 860 Imaging Analysis System from Amersham Biosciences and quantified using ImageQuant. Untreated transfected cells were also collected as control for the expression of FLAG–SMS1 or FLAG–SMS2 by Western blot and for SMS activity.

bSMase (bacterial SMase) treatment and SM re-synthesis

HeLa cells were plated in 10-cm-diameter dishes at a density of 0.3×10^6 for overexpression of FLAG–SMS1 or FLAG–SMS2. After 24 h of overexpression, cells were washed with growth medium and then treated with 50 mU/ml bSMase for 60 min. The medium was then removed and cells were washed three times with PBS. After addition of fresh growth medium, the cells were incubated for the indicated time. Cells were then collected and non-radioactive measurement of SM mass levels was performed as previously described [6]. The expression of FLAG–SMS1 and FLAG–SMS2 was confirmed by SMS *in vitro* activity for each experiment.

Immunofluorescence and confocal microscopy

HeLa cells were plated in 35-mm-diameter confocal dishes at a density of 5×10^4. After 24 h, cells were transfected with 1 μg of pcDNA3.1 plasmid carrying a conventional C1 domain mutated to increase its binding affinity for DAG (YFP–DBD; yellow fluorescent protein–DAG-binding domain) provided by Dr Alexandra Newton (University of California, San Diego, CA, U.S.A.) [25]. After 22 h of transfection, the medium was replaced and cells were treated with 20 nM PMA for 30 min, 10 μM DiC8 (1,2-dioctanoyl-*sn*-glycerol) for 1 h, 3 μM D-e-C_6-ceramide or L-e-C_6-ceramide (where e is *erythro*) for 1 h in growth medium. For down-regulation of SMSs, cells were plated at a density of 3×10^4 in 35-mm-diameter confocal dishes. After 24 h, cells were treated with 10 nM siRNA or Oligofectamine™ alone (control). After 48 h, cells were transfected with 1 μg of YFP–DBD plasmid as described above and incubated for 22 h. In some experiments, 1 μg of PKD–RFP (PKD–red fluorescent protein), provided by Dr O. Rey and Dr E. Rozengurt (David Geffen School of Medicine, University of California, Los Angeles, CA, U.S.A.) was transfected instead for 16 h using Superfect reagent from Qiagen according to the manufacturer's instructions. Cells were then treated as required. In the case of bSMase treatment, 50 mU/ml bSMase was incubated with the cells for 1 h, then bSMase was washed off, and cells were incubated with regular growth medium for an additional 3 h. Treatments were stopped by fixation with

3.7% formaldehyde for 15 min at room temperature (24 °C). After washing the plates with PBS, the cells were analysed by confocal microscopy. Confocal images were captured and processed using an LSM 510 META laser-scanning microscope (Zeiss, Jena, Germany). In some experiments, HeLa cells were co-transfected with 1 μg each of YFP–DBD and pcDNA 3.1 (empty vector), SMS1–FLAGor SMS2–V5 for 22 h and then treated with 3 μM C_6-ceramide. After fixation with 3.7% formaldehyde for 15 min at room temperature, cells were permeabilized with 100% methanol (−20°C) for 5 min. Cells were washed three times with 1.5% FBS in PBS for 5 min each and then blocked in 2.5% FBS for 1 h at room temperature. Incubation with the primary antibody was performed using mouse monoclonal anti-V5 or anti-FLAG antibodies (from Invitrogen and Sigma respectively) in 1.5% FBS in PBS with 0. 5% saponin at 1:100 dilution for 1.5 h at room temperature. Cells were then washed three additional times with 1.5% FBS/PBS for 5 min each and incubated with anti-mouse Alexa Fluor® 633-conjugated antibodies (1:400 in 1.5% FBS in PBS with 0.5% saponin) for 1 h at room temperature in the dark. Cells were washed three additional times with 1.5% FBS/PBS for 5 min each before analysis at the confocal microscope. In some experiments, giantin and TGN38 (*trans*-Golgi network protein 38) were used as Golgi markers. Anti-giantin antibodies from Covant were used at 1:200 dilution, whereas anti-TGN38 antibodies from Santa Cruz were used at 1:50 dilution. Alexa Fluor® 633- or 488-conjugated anti-rabbit or anti-goat antibodies were used as secondary antibodies. In the experiments with SV40-transformed WI38 cells, 0.025×10^6 cells were plated in uncoated confocal dishes. After 48 h, cells were treated with 50 nM siRNA. After 48 h of down-regulation, cells were transfected with 1 μg of YFP–DBD using Effectene® reagent from Qiagen according to the manufacturer's instructions. After 16 h, cells were treated with 3 μM C_6-ceramide and then processed accordingly.

YFP–DBD fractionation

HeLa cells were plated in 10-cm-diameter dishes at a density of 0.2×10^6, with four plates for each treatment group. After 48 h, cells were transfected with 0.2–0.5 μg of the mammalian expression plasmid carrying YFP–DBD. After 16 h, cells were treated with 3 μM C_6-ceramide for 1 h and then collected by scraping in PBS. Cells were lysed by sonication (three cycles of 15 s with 30 s intervals in between). An aliquot was used for detection of total YFP–DBD and the rest was spun at 1000 ***g*** for 10 min to separate nuclei. Post-nuclear lysate was centrifuged at 100000 ***g*** for 1 h at 4°C. Total membrane fractions were resuspended in sample buffer and used for Western blotting. Aliquots of total lysate from each sample with approximately the same level of transfected YFP–DBD were loaded on an SDS/10% PAGE gel. Aliquots of total membranes corresponding to the fraction of total lysate used were loaded alongside. Gels were transferred on to nitrocellulose membranes which were then blotted with anti-GFP/YFP monoclonal antibodies (Clontech; 1:1000 dilution). The signal was detected after blotting the membranes with HRP (horseradish peroxidase)-conjugated anti-mouse secondary antibodies (1:6000) and developed by ECL® (enhanced chemiluminescence) (Amersham). The intensity of the signal was determined by densitometry using Labworks software.

Statistical analysis

Statistical analysis of the data was performed using Student's *t*-test, and $P < 0.05$ was considered statistically significant.

RESULTS

Effectiveness and specificity of modulation of SMS1 or SMS2

In order to characterize the role of human SMS1 and SMS2 in the formation of DAG, lipid analysis was conducted upon modulation of the two enzymes by down- or up-regulation of their expressions by transiently transfecting cells with siRNA or SMS expression plasmids. Because this study was initiated prior to the publication of other recent studies in which siRNA was also used [22,23], this resulted in different siRNA sequences being used in the present study from the published ones. Therefore a thorough analysis of their effectiveness and specificity was carried out. As illustrated in the Supplementary material section (at http://www.BiochemJ.org/bj/414/bj4140031add.htm) in Supplementary Figure S1, both siRNA sequences were effective and specific in down-regulating each SMS. Down-regulation or up-regulation of SMS1 or SMS2 reduced or enhanced *de novo* synthesis of SM (Supplementary Figure S2), and SM mass levels (Supplementary Figure S3) respectively. Down-regulation of either SMS resulted in increased ceramide levels (Supplementary Figure S4). These results demonstrate the effectiveness and specificity of the experimental model used in this study to modulate SMS expression.

Down-regulation of SMS1 or SMS2 does not affect total basal DAG levels

Studies conducted in mammalian cells by us (Supplementary material) and others [7,18,20–23] have confirmed the ability of both SMSs to regulate the levels of SM and ceramide in cells. On the other hand, no published clear evidence for involvement of SMS1 or SMS2 in the regulation of DAG exists. Therefore it was investigated if down-regulation of SMS1 or SMS2 could also affect the endogenous levels of this bioactive lipid. Interestingly, as shown in Figure 1(A), down-regulation of neither SMS1 nor SMS2 caused significant changes in total DAG levels as measured by the DGK assay.

SMS1 and SMS2 produce DAG *in vitro*

Since no significant changes in the basal levels of both PC (putative substrate) and DAG (putative product) were observed upon down-regulation of either SMS, the ability of the two SMSs to use PC as substrate to form DAG, after their expression in mammalian cells, was determined *in vitro*. After 24 h of overexpression, both FLAG–SMSs were able to produce NBD-C_6-(Figure 1B) or NBD-C_{12}-DAG (Figure 1C) from NBD-C_6- or NBD-C_{12}-PC respectively with an activity profile similar to the one obtained using NBD-C_6-ceramide as substrate (Supplementary Figure S1D). These results confirm the ability of SMS1 and SMS2 to form DAG from PC, at least in an *in vitro* setting.

SMS1 and SMS2 are able to regulate formation of DAG

Because no changes of total DAG levels were observed under basal conditions upon SMSs down-regulation (Figure 1A), whereas both SMSs could use PC as substrate to form DAG *in*

vitro (Figures 1B and 1C), the possibility that SMSs could modulate subcellular pools of DAG once acute activation of the enzymes is triggered was investigated.

To address this point, YFP–DBD was used to probe subcellular pools of DAG in the cells [25]. Stimulation of SM synthesis was first induced by treatment with short-chain ceramide analogues which have been widely used as a substrate for studying SM synthesis in cells [15,26]. In order to verify that both SMS1 and SMS2 use these ceramide analogues as substrates once they enter the cells, HeLa cells were treated with NBD-C_6-ceramide after modulation of SMSs (Figure 2). After SMS1 and SMS2 down-regulation (10 nM SMS1 or SMS2 siRNA for 48 h), HeLa cells were treated with 5 μM NBD-C_6-ceramide for 4 h, and the effect of down-regulation of SMSs on the conversion of NBD-C_6-ceramide into NBD-C_6-SM was determined. As shown in Figure 2(A), down-regulation of SMS1 (SMS1−) or SMS2 (SMS2−) induced a significant decrease in the amount of NBD-C_6-SM produced by approx. 70 and 40% respectively. Importantly, no decrease in the production of NBD-C_6-glucosylceramide was observed (results not shown), supporting, also in this case, the specificity of the effects elicited by the selected SMS1 and SMS2 siRNA. Similar results were obtained at 2, 6 and 8 h of NBD-C_6-ceramide incubation (results not shown). On the other hand, 24 h of overexpression of FLAG–SMS1 or FLAG–SMS2 significantly enhanced cellular synthesis of NBD-C_6-SM from NBD-C_6-ceramide at 4 h (Figure 2B). Interestingly, the enhancement of NBD-C_6-SM production induced a slight decrease of NBD-C_6-glucosylceramide production, suggesting possible competition for substrate (the same profile was obtained at 2, 6 and 8 h of treatment as well as after 36 h of overexpression; results not shown). Thus these results demonstrate that short-chain ceramide analogues are used as substrate in cells by both SMSs. Moreover, since NBD-C_6-ceramide is known to be delivered and metabolized to the Golgi, these data also suggest that the fraction of SMS2 present in this compartment has significant SMS activity.

To ascertain that the YFP–DBD is indeed able to respond to changes in the levels of DAG or DAG analogues in the cell, HeLa cells were transfected with YFP–DBD and then loaded with functional analogues of DAG (PMA or DiC8) [16]. Although control cells showed both a diffuse and perinuclear punctate pattern of the YFP–DBD (Figure 3A), cells treated with PMA (Figure 3B) showed a clear and expected translocation of the YFP–DBD to the plasma membrane, whereas treatment with DiC8 induced translocation of the YFP–DBD to a juxtanuclear subcellular compartment consistent with the Golgi apparatus (Figure 3C). These results clearly show the responsiveness of the YFP–DBD to changes in DAG analogue levels within the cells. Once the system proved to be functional, the localization of the YFP–DBD in conditions of stimulated SM synthesis was addressed. Because of the ability of short-chain ceramide analogues to be recognized as SMS substrates (Figure 2), induction of SM synthesis in YFP–DBD expressing cells was stimulated by treatment with C_6-ceramide (Figure 3D). In response to such treatment, YFP–DBD co-localized with the Golgi marker giantin (Figures 3E and 3F), indicating the translocation of the YFP–DBD in the Golgi, a known subcellular site for SM synthesis. In order to make sure that the translocation of the YFP–DBD to the Golgi in ceramide-treated cells was due to metabolism of ceramide and not to the presence of ceramide itself, cells were treated with L-e-C_6-ceramide, a stereoisomer that is not metabolized in the cells [26] (Figure 3I). In this case, no significant difference between control (Figure 3G) and L-e-C_6-ceramide treated cells was

observed (Figure 3I), suggesting that translocation of YFP–DBD is due to ceramide metabolism in the Golgi. Importantly, the site of YFP–DBD translocation when SM synthesis is stimulated corresponded not only to the Golgi (Figure 3F) but also to the site of cellular localization of SMS1 (Figures 4A–4C) and, in part, of SMS2 (Figures 4D–4F). Altogether these results suggest that SM synthesis, stimulated by metabolism of C_6-ceramide, induces translocation of YFP–DBD through formation of DAG at the Golgi site where SMSs reside.

In order to investigate whether SMSs were responsible for the translocation of YFP–DBD under conditions of active SM synthesis in the Golgi, the effect of knockdown of SMS1 and SMS2 on YFP–DBD translocation induced by treatment with C_6-ceramide was determined (Figure 5). As shown in the Figure, down-regulation of SMS1 (Figure 5C) or SMS2 (Figure 5D) did not induce significant changes in the juxtanuclear pattern of the YFP–DBD under unstimulated conditions. On the other hand, upon stimulation with D-e-C_6-ceramide, knockdown of SMS1 (Figure 5G) induced a significant loss of translocation of the YFP–DBD to the Golgi as compared with Oligofectamine™ (Figure 5E) or SCR (Figure 5F) controls. A less pronounced, yet still present, inhibition of the translocation of YFP–DBD was observed upon knockdown of SMS2 (Figure 5H). In order to confirm and quantify the effect of down-regulation of SMS1 and SMS2 on the translocation of YFP–DBD, total membrane fractions were isolated after downregulation of either SMSs, transfection with YFP–DBD and C_6-ceramide treatment. Total cell extracts and respective total membrane fractions were loaded on an SDS gel and the YFP–DBD levels were determined by Western blotting (Figure 6A). As shown in Figure 6(B), quantification of the levels of YFP–DBD present in the membrane fractions over the total YFP–DBD present in each sample revealed a 4-fold reduction of YFP–DBD in the membrane fraction upon SMS1 down-regulation. Less prominent but still significant was the effect of down-regulation of SMS2. Similar results were also obtained in human SV40-transformed WI38 lung fibroblasts as shown by analysis using the confocal microscope (Figures 7 and 8). Also in this cell line, in non-stimulated conditions, downregulation of either SMS1 or SMS2 did not significantly alter the diffuse pattern of YFP–DBD within the cell (results not shown), whereas treatment with C6-ceramide enhanced localization of YFP–DBD to the Golgi, as shown by its co-localization with the Golgi markers giantin and TGN38 (Figure 7). On the other hand, downregulation of SMS1 clearly inhibited the Golgi localization of YFP–DBD induced by stimulation of SM synthesis with C6-ceramide (Figure 8C). Similar to HeLa, also in SV40-transformed WI38 cells the effect of downregulation of SMS2 was less pronounced than that observed upon SMS1 knock-down but still appreciable (Figure 8D). In order to confirm further these results, two additional specific and effective siRNAs targeting *SMS2* [22,23] were also employed (SMS2.2− and SMS2.3−) (Figures 8E and 8F). Importantly, these additional siRNAs confirmed the results obtained with the original SMS2− sequence (Figure 8D). Altogether, these results support the hypothesis that SMS1 and, less pronouncedly, SMS2 are able to modulate DAG formation at the Golgi.

To investigate further the ability of SMS1 or SMS2 to regulate DAG formation using endogenous substrates, stimulation of SM synthesis was triggered by increasing ceramide levels through SM hydrolysis induced by acute treatment with bSMase of intact HeLa cells. As shown in Figures 9(A) and 9(B), 1 h of treatment with bSMase caused the hydrolysis of

approx. 60% of total SM, and once the bSMase was washed off, the cells resynthesized SM up to approx. 85% of control levels within 4 h. Overexpression of either SMS1 or SMS2 induced a significant increase of SM resynthesis, allowing more than double the amount of SM to be produced in 2.5 h compared with vector control (approx. 17 nmol of SM/nmol of P_i for SMSs compared with 7 nmol of SM/nmol of P_i for vector) (Figure 9C). These results suggest that both SMS1 and SMS2 contribute to SM synthesis from ceramide produced at the plasma membrane. In order to evaluate whether stimulation of SM synthesis from endogenous ceramide would induce formation of DAG, the localization of YFP–DBD was determined in cells treated with bSMase and allowed to re-synthesize SM for 3 h. As shown in Figures 10(A) and 10(B), SM synthesis from plasma membrane ceramide induced translocation of YFP–DBD to the Golgi (Figures 10A and 10B compared with Figures 5A and 5B). Importantly, down-regulation of either SMS1 or SMS2 significantly inhibited the translocation of YFP–DBD, causing a more diffuse localization similar to control cells (Figures 10C and 10D compared with Figures 5C and 5D). Altogether, these results suggest that the bulk of ceramide generated at the plasma membrane is routed to the Golgi for SM resynthesis, that both SMS1 and SMS2 at the Golgi are responsible for SM resynthesis to occur and that both SMS1 and SMS2 are capable of DAG formation at the Golgi using endogenous ceramide.

In order to assess the biological functionality of the production of DAG through SMS1 and SMS2 at the Golgi, the effect of stimulation of SM synthesis on the localization of the DAG-binding protein PKD was determined. Stimulation of SM synthesis was triggered by treatment with C_6-ceramide and it was found to enhance localization of PKD–RFP to a perinuclear region resembling the Golgi apparatus (compare Figure 11A with Figure 11B or 11E). To confirm the enhanced localization of PKD–RFP to the Golgi upon stimulation of SM synthesis, cells transiently trasfected with PKD–RFP and treated with C_6-ceramide were stained with the Golgi markers giantin (Figures 11B–11D) or TGN38 (Figures 11E–11G). Indeed the co-localization of PKD–RFP with the Golgi markers after treatment with C_6-ceramide suggests the relocalization of PKD–RFP to the site of SM synthesis. Importantly, down-regulation of SMS1 clearly inhibited localization of PKD–RFP to the Golgi (Figure 12C compared with 12A and 12B), with PKD–RFP scattered throughout the cell similarly to control cells (Figure 11A). Comparable with what was observed in the case of YFP–DBD, the effect of down-regulation of SMS2 with all three different siRNA sequences used (Figures 12D–12F) was less prominent than that observed after knockdown of SMS1. Overall, these results support the conclusion that SMS1 and, to a lesser extent, SMS2 are able to produce DAG at the Golgi, and that this DAG is biologically active since it is able to recruit DAG-binding proteins such as PKD to this organelle.

DISCUSSION

In the present study we provide direct evidence that both SMS1 and SMS2 possess the ability of regulating the production of DAG at the Golgi, and that this pool of DAG is biologically active.

One of the proposed relevant biochemical features of the SMS class of enzymes is the formation of DAG. This biochemical characteristic would make SMS a potentially important

regulator for the cross-talk between sphingolipids and glycerolipids. Interestingly, whereas we show that FLAG-tagged SMSs expressed in mammalian cells use PC to produce DAG *in vitro*, we find that down-regulation of either SMS did not lower the total cellular mass of DAG as measured by the DGK assay. This observation is in agreement with other recently published results [22,23], and it might indicate one of the following possibilities: (i) SMSs recognize a very selective endogenous pool of PC, thus producing a specific pool of DAG measurable only by more discriminating methods of detection such as MS; (ii) the endogenous substrate for SMSs is not PC; (iii) alternative pathways that lead to the formation of DAG promptly compensate for the loss of this lipid mediated by down-regulation of SMSs; this possibility would complement a report describing that no accumulation of DAG from SM synthesis can be observed in certain cell lines because of its back-conversion into PC [27] thus suggesting that, in certain cellular settings, the levels of DAG regulated by SMS are strictly controlled.

On the other hand, the use of the YFP–DBD in combination with treatments that stimulate SM synthesis allowed us to visualize the ability of SMS1 and SMS2 to modulate DAG levels at the Golgi. The responsiveness of this mutated C1 domain to localized elevation of DAG was shown in COS-7 cells in response to UTP treatment [25]. In our system, the YFP–DBD proved extremely useful to probe changes in acute localized production of DAG upon down-regulation of SMS1 or SMS2. The acute stimulation of SM synthesis with either C_6-ceramide or short-term bSMase treatment was key to the success of this approach since there was no significant difference in DAG distribution under basal conditions when SMS1 and SMS2 were down-regulated. This could be due to the fact that the acute stimulation did not allow other metabolic pathways to compensate at the level of control cells for the loss of DAG due to SMS down-regulation.

The observation that SMSs may regulate DAG at the Golgi implicates them in the regulation of DAG-binding proteins known to respond to DAG metabolism in this compartment through the presence of a C1 domain [28], such as novel PKCs or PKD [16]. The latter, in particular, was found to translocate to the Golgi in response to sphingolipid synthesis, possibly through the formation of DAG by SMS [16]. Indeed we show that knockdown of SMS1 and, to a lesser extent, of SMS2, while causing a decrease of DAG formation in the Golgi (as visualized through the YFP–DBD), also caused inhibition of the localization of PKD to this compartment. The herein reported ability of SMSs to produce DAG provides the first direct evidence for the link between Golgi-localized SMSs and PKD and thus, ultimately, for the regulation of secretion by SMSs. On the other hand, the translocation of PKD to the Golgi was found to feed back negatively on SM synthesis through inactivation of CERT (ceramide transfer protein), which in turn is critical for PKD activation, demonstrating a very tight connection among SM metabolism, PKD activity and regulation of secretion [29].

Even though evidence in the present study supports the notion that SMS2 localized at the Golgi exerts significant SMS activity (see effects on *de novo* synthesis of SM presented in Supplementary Figure S2 and on NBD-C_6-ceramide metabolism presented in Figure 2), we observed a considerably milder role for endogenous SMS2 on production and activity of DAG at the Golgi as compared with SMS1. This difference could be simply be a function of

the overall lower activity of SMS2 compared with SMS1 in the Golgi which leads to an insufficient amount of DAG produced or to the possibility that SMS1 and SMS2 have different PC substrate specificity and generate different DAG pools with different biological activities or that the pool of DAG produced by SMS1 is more accessible to DAG-binding proteins in the cytosol.

In conclusion, we have shown that SMS1 and, to a lesser extent, SMS2 possess the ability of regulating the production of DAG at the Golgi, and that this pool of DAG is biologically active. These results open up a series of important questions on the function of SMS1 and SMS2 in the regulation of DAG production in response to specific stimuli, on the endogenous source of the phosphorylcholine headgroup and on the reciprocal regulation of SMS1 compared with SMS2. It is our intention to contribute to finding answers to some of these questions with our ongoing studies.

While this manuscript was under revision, a study confirming that down-regulation of either SMS1 or SMS2 is able to regulate DAG levels was published [30]. The fact that in the cell line used in that manuscript showed downregulation of SMSs determined a difference on total DAG levels whereas HeLa cells did not show such a response, indicate that different cell types react differently to perturbation of DAG metabolism.

Supplementary Material

Refer to Web version on PubMed Central for supplementary material.

Acknowledgments

We are grateful to Dr Yusuf Hannun and Dr Lina Obeid for their enthusiastic support and critical discussion. We thank the Biotechnology Resource Laboratory and the Hollings Cancer Center at the Medical University of South Carolina for their support with DNA sequencing and imaging analysis respectively. This work was supported in part by the National Science Foundation/EPSCoR under grant EPS-0132573, by a Hollings Cancer Center/Medical University of South Carolina Department of Defense grant Translational Research on Cancer Control and Related Therapy (Subcontract GC-3319-05-4498CM), by NIH (National Institutes of Health) grant P20 RR-017677 from the National Center for Research Resources, and by grant IRG 97-219-08 from the American Cancer Society. M. Del P. is a Burroughs Wellcome New Investigator in the Pathogenesis of Infectious Diseases.

Abbreviations used

bSMase	bacterial sphingomyelinase
DAG	diacylglycerol
DBD	DAG-binding domain
DGK	diacylglycerol kinase
DiC8	1,2-dioctanoyl-*sn*-glycerol
DMEM	Dulbecco’s modified Eagle’s medium
FBS	fetal bovine serum
NBD	*N*-(7-nitrobenz-2-oxa-1,3-diazol-4-yl)

PC	phosphatidylcholine
PKC	protein kinase C
PKD	protein kinase D
RFP	red fluorescent protein
SCR	scrambled siRNA
siRNA	short interfering RNA
SM	sphingomyelin
SMS	SM synthase
SV40	simian virus 40
TGN38	*trans*-Golgi network protein 38
YFP	yellow fluorescence protein.

REFERENCES

1. Ullman MDR, Radin N. The enzymatic formation of sphingomyelin from ceramide and lecithin in mouse liver. J. Biol. Chem. 1974; 249:1506–1512. [PubMed: 4817756]
2. Bernert JT, Ullman MD. Biosynthesis of sphingomyelin from erythro-ceramides and phosphatidylcholine by a microsomal cholinephosphoesterase. Biochim. Biophys. Acta. 1981; 666:99–109. [PubMed: 6271237]
3. Marggraf WD, Anderer FA, Kanfer J. The formation of sphingomyelin from phosphatidylcholine in plasma membrane preparations from mouse fibroblasts. Biochim. Biophys. Acta. 1981; 664:61–73. [PubMed: 6263341]
4. Marggraf WD, Zertani R, Anderer FA, Kanfer JN. The role of endogenous phosphatidylcholine and ceramide in the biosynthesis of sphingomyelin in mouse fibroblasts. Biochim. Biophys. Acta. 1982; 710:314–323. [PubMed: 6280771]
5. Voelker DRK, Kennedy EP. Cellular and enzymic synthesis of sphingomyelin. Biochemistry. 1982; 21:2753–2759. [PubMed: 7093220]
6. Luberto C, Hannun YA. Sphingomyelin synthase, a potential regulator of intracellular levels of ceramide and diacylglycerol during SV40-transformation: does sphingomyelin synthase account for the putative phosphatidylcholine-phospholipase C? J. Biol. Chem. 1998; 273:14550–14559. [PubMed: 9603970]
7. Miyaji M, Jin ZX, Yamaoka S, Amakawa R, Fukuhara S, Sato SB, Kobayashi T, Domae N, Mimori T, Bloom ET, et al. Role of membrane sphingomyelin and ceramide in platform formation for Fas-mediated apoptosis. J. Exp. Med. 2005; 202:249–259. [PubMed: 16009715]
8. Gulbins E, Kolesnick R. Raft ceramide in molecular medicine. Oncogene. 2003; 22:7070–7077. [PubMed: 14557812]
9. Miro-Obradors M-J, Osada J, Aylagas H, Sanchez-Vegazo I, Palacios-Alaiz E. Microsomal sphingomyelin accumulation in thioacetamide-injured regenerating rat liver: involvement of sphingomyelin synthase activity. Carcinogenesis. 1993; 14:941–946. [PubMed: 8389255]
10. Riboni L, Viani P, Bassi R, Giussani P, Tettamanti G. Basic fibroblast growth factor-induced proliferation of primary astrocytes: evidence for the involvement of sphingomyelin biosynthesis. J. Biol. Chem. 2001; 276:12797–12804. [PubMed: 11278937]
11. Bourteele S, Hausser A, Doppler H, Horn-Muller J, Ropke C, Schwarzmann G, Pfizenmaier K, Muller G. Tumor necrosis factor induces ceramide oscillations and negatively controls

sphingolipid synthases by caspases in apoptotic Kym-1 cells. J. Biol. Chem. 1998; 273:31245–31251. [PubMed: 9813032]

12. Watanabe M, Kitano T, Kondo T, Yabu T, Taguchi Y, Tashima M, Umehara H, Domae N, Uchiyama T, Okazaki T. Increase of nuclear ceramide through caspase-3-dependent regulation of the “sphingomyelin cycle” in Fas-induced apoptosis. Cancer Res. 2004; 64:1000–1007. [PubMed: 14871831]
13. Cerbon J, del Carmen Lopez-Sanchez R. Diacylglycerol generated during sphingomyelin synthesis is involved in protein kinase C activation and cell proliferation in Madin-Darby canine kidney cells. Biochem. J. 2003; 373:917–924. [PubMed: 12691604]
14. Meng A, Luberto C, Meier P, Bai A, Yang X, Hannun YA, Zhou D. Sphingomyelin synthase as a potential target for D609-induced apoptosis in U937 human monocytic leukemia cells. Exp. Cell Res. 2004; 292:385–392. [PubMed: 14697345]
15. Luberto C, Yoo DS, Suidan HS, Bartoli GM, Hannun YA. Differential effects of sphingomyelin hydrolysis and resynthesis on the activation of NF-κB in normal and SV40-transformed human fibroblasts. J. Biol. Chem. 2000; 275:14760–14766. [PubMed: 10799564]
16. Baron CL, Malhotra V. Role of diacylglycerol in PKD recruitment to the TGN and protein transport to the plasma membrane. Science. 2002; 295:325–328. [PubMed: 11729268]
17. Huitema K, Van Den Dikkenberg J, Brouwers JF, Holthuis JC. Identification of a family of animal sphingomyelin synthases. EMBO J. 2004; 23:33–44. [PubMed: 14685263]
18. Yamaoka S, Miyaji M, Kitano T, Umehara H, Okazaki T. Expression cloning of a human cDNA restoring sphingomyelin synthesis and cell growth in sphingomyelin synthase-defective lymphoid cells. J. Biol. Chem. 2004; 279:18688–18693. [PubMed: 14976195]
19. Futerman AH, Pagano RE. Determination of the intracellular sites and topology of glucosylceramide synthesis in rat liver. Biochem. J. 1991; 280:295–302. [PubMed: 1747103]
20. van der Luit AH, Budde M, Zerp S, Caan W, Klarenbeek JB, Verheij M, van Blitterswijk WJ. Resistance to alkyl-lysophospholipid-induced apoptosis due to downregulated sphingomyelin synthase 1 expression with consequent sphingomyelin-and cholesterol-deficiency in lipid rafts. Biochem. J. 2007; 401:541–549. [PubMed: 17049047]
21. Dong J, Liu J, Lou B, Li Z, Ye X, Wu M, Jiang XC. Adenovirus-mediated overexpression of sphingomyelin synthases 1 and 2 increases the atherogenic potential in mice. J. Lipid Res. 2006; 47:1307–1314. [PubMed: 16508036]
22. Tafesse FG, Huitema K, Hermansson M, van der Poel S, van den Dikkenberg J, Uphoff A, Somerharju P, Holthuis JC. Both sphingomyelin synthases SMS1 and SMS2 are required for sphingomyelin homeostasis and growth in human HeLa cells. J. Biol. Chem. 2007; 282:17537–17547. [PubMed: 17449912]
23. Li Z, Hailemariam TK, Zhou H, Li Y, Duckworth DC, Peake DA, Zhang Y, Kuo MS, Cao G, Jiang XC. Inhibition of sphingomyelin synthase (SMS) affects intracellular sphingomyelin accumulation and plasma membrane lipid organization. Biochim. Biophys. Acta. 2007; 1771:1186–1194. [PubMed: 17616479]
24. Bligh EG, Dyer WJ. A rapid method of total lipid extraction and purification. Can. J. Biochem. Physiol. 1959; 37:911–917. [PubMed: 13671378]
25. Dries DR, Gallegos LL, Newton AC. A single residue in the C1 domain sensitizes novel protein kinase C isoforms to cellular diacylglycerol production. J. Biol. Chem. 2007; 282:826–830. [PubMed: 17071619]
26. Venkataraman K, Futerman AH. Comparison of the metabolism of L-erythro- and L-threo-sphinganines and ceramides in cultured cells and in subcellular fractions. Biochim. Biophys. Acta. 2001; 1530:219–226. [PubMed: 11239824]
27. Sillence DJ, Allan D. Utilization of phosphatidylcholine and production of diradylglycerol as a consequence of sphingomyelin synthesis. Biochem. J. 1998; 331:251–256. [PubMed: 9512487]
28. Carrasco S, Merida I. Diacylglycerol, when simplicity becomes complex. Trends Biochem. Sci. 2007; 32:27–36. [PubMed: 17157506]
29. Fugmann T, Hausser A, Schoffler P, Schmid S, Pfizenmaier K, Olayioye MA. Regulation of secretory transport by protein kinase D-mediated phosphorylation of the ceramide transfer protein. J. Cell. Biol. 2007; 178:15–22. [PubMed: 17591919]

30. Ding T, Li Z, Hailemariam T, Mukherjee S, Maxfield FR, Wu MP, Jiang XC. SMS overexpression and knockdown: impact on cellular sphingomyelin and diacylglycerol metabolism, and cell apoptosis. J. Lipid Res. 2008; 49:376–385. [PubMed: 17982138]

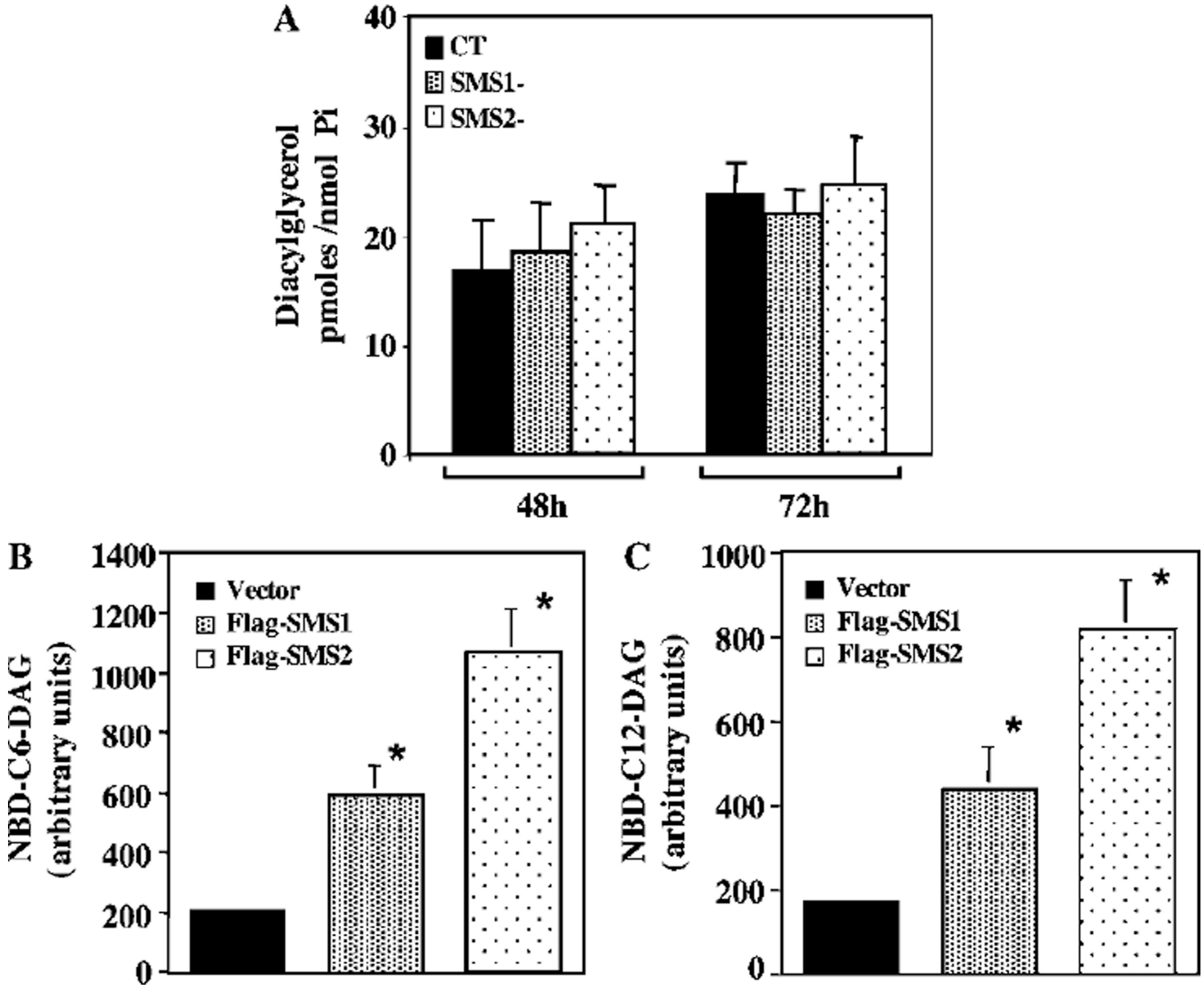

Figure 1. SMS1 and SMS2 regulate DAG production *in vitro* but their downregulation does not affect basal total DAG levels

(**A**) Cells were treated with siRNA targeting *SMS1* (SMS1−) or *SMS2* (SMS2−) for 48 or 72 h and then collected for DAG determination by DGK assay. The results shown are the means of two independent experiments performed in duplicate. Error bars represent S.D. (**B** and **C**) Cells were transfected with empty vector, FLAG–SMS1 or FLAG–SMS2 for 24 h. Cells were then collected and processed for *in vitro* SMS enzymatic assay as described in the Experimental section. Fluorescently-labelled short-chain PC analogues (NBD-C_6-PC or NBD-C_{12}-PC) were used as substrates. The results shown are the means for three independent experiments. Error bars represent S.D. and $*P < 0.05$ compared with vector.

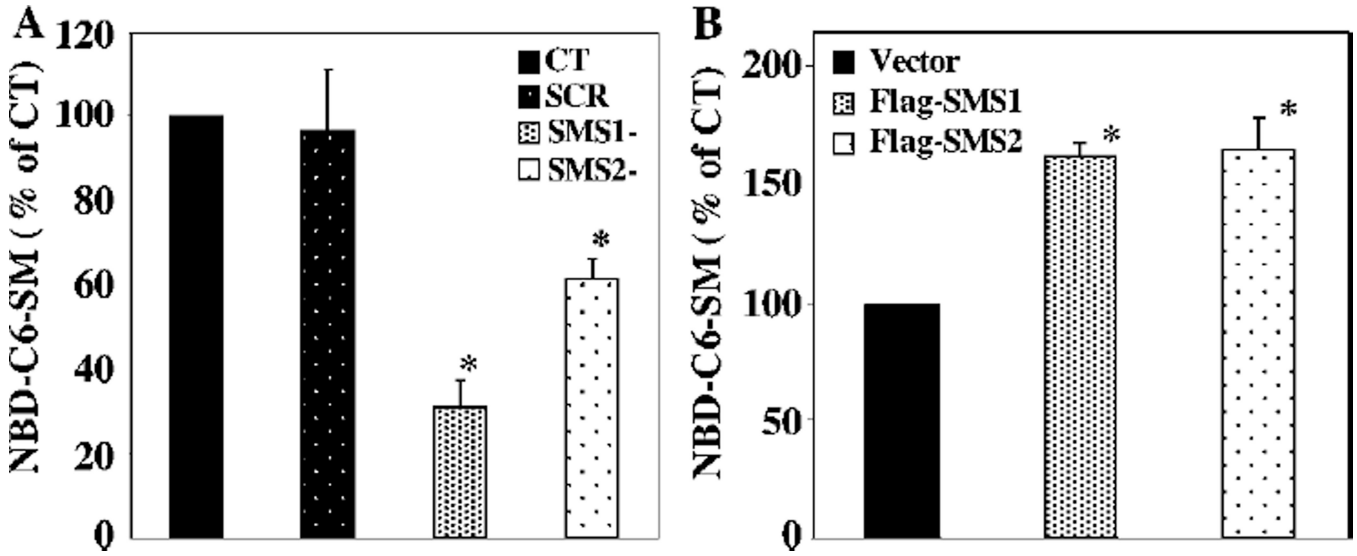

Figure 2. Modulation of SMS1 or SMS2 affects cellular metabolism of NBD-C_6-ceramide to NBD-C_6-SM

(**A**) HeLa cells were treated with Oligofectamine™ alone (CT), with 10 nM SCR or siRNA targeting *SMS1* (SMS1−) or *SMS2* (SMS2−) for 48 h. (**B**) Cells were transfected with empty vector, FLAG–SMS1 or FLAG–SMS2 for 24 h. HeLa cells were then treated with 5 μM NBD-C_6-ceramide for 4 h, and total lipids were extracted as described by Bligh and Dyer [24]; equal amount of total phospholipids were loaded on to a TLC plate and lipids were separated in chloroform/methanol/15mM $CaCl_2$ (60:35:8, by vol.). Fluorescent lipids were visualized using a phosphorimager and identified using authentic standards. The results are the means for at least three independent experiments, and error bars represent S.D. and $*P < 0.05$ compared with Oligofectamine™ alone (**A**) or vector control (**B**).

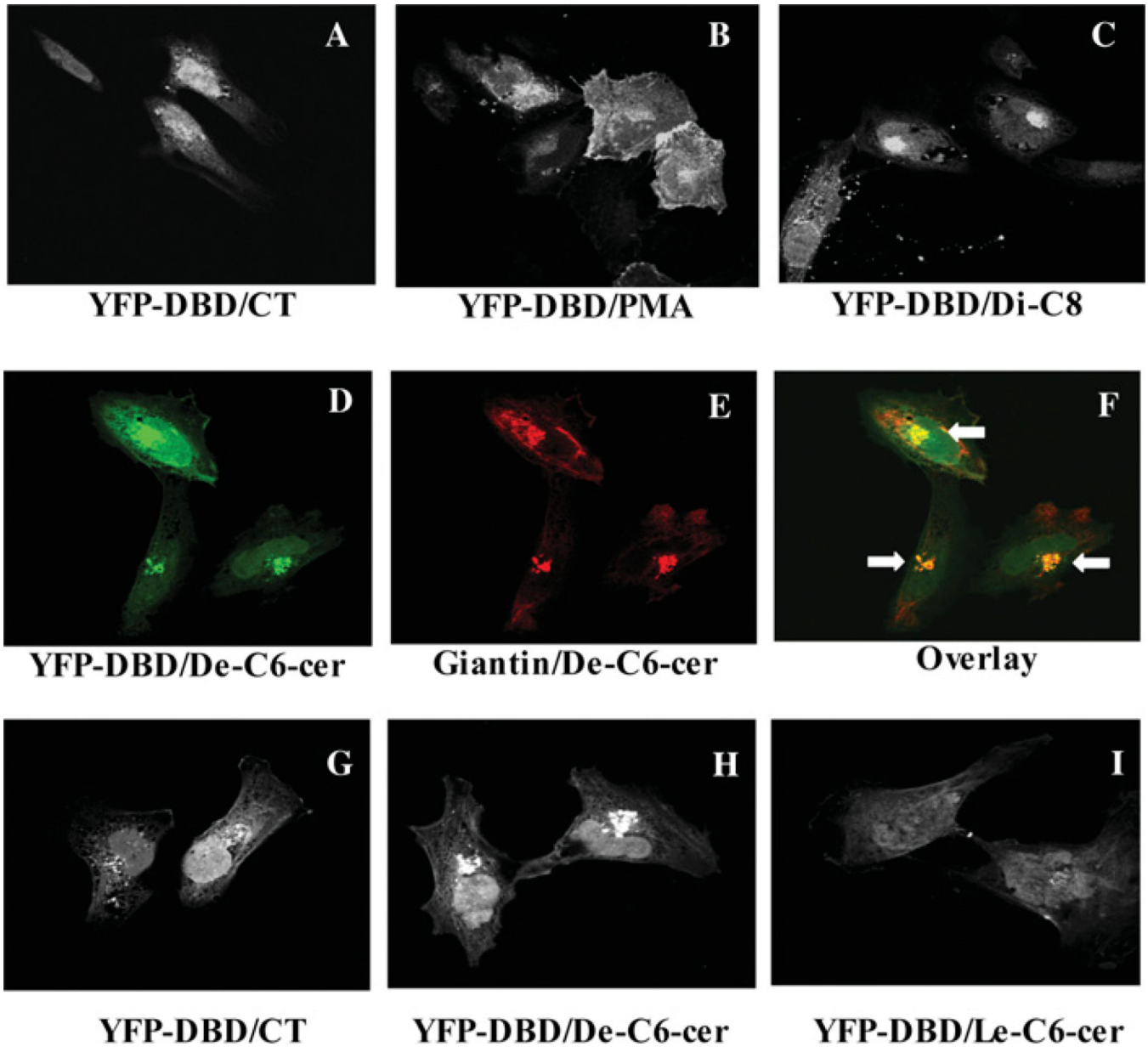

Figure 3. Metabolism of short-chain ceramide induces production of DAG at the Golgi

HeLa cells were transfected with 1 μg of YFP–DBD for 22 h. Then cells were either left untreated (**A**) and (**G**) or treated with 20 nM PMA for 30 min (**B**) or with 10 μM DiC8 (**C**), with 3 μM D-e-C_6-ceramide (**D**), (**E**) and (**H**) or 3 μM L-e-C_6-ceramide (**I**) for 1 h. Cells were fixed, and in (**A–C**) and (**G–I**), cells were analysed directly by confocal microscopy using the YFP fluorescence. Confocal images were captured and processed using LSM 510 META. In (**D–F**), cells were processed for indirect immunofluorescence with anti-giantin (Golgi marker) polyclonal antibodies and stained with anti-rabbit Alexa Fluor® 633-conjugated secondary antibodies (red). Images are representative of at least two independent experiments. Arrows indicate sites of co-localization.

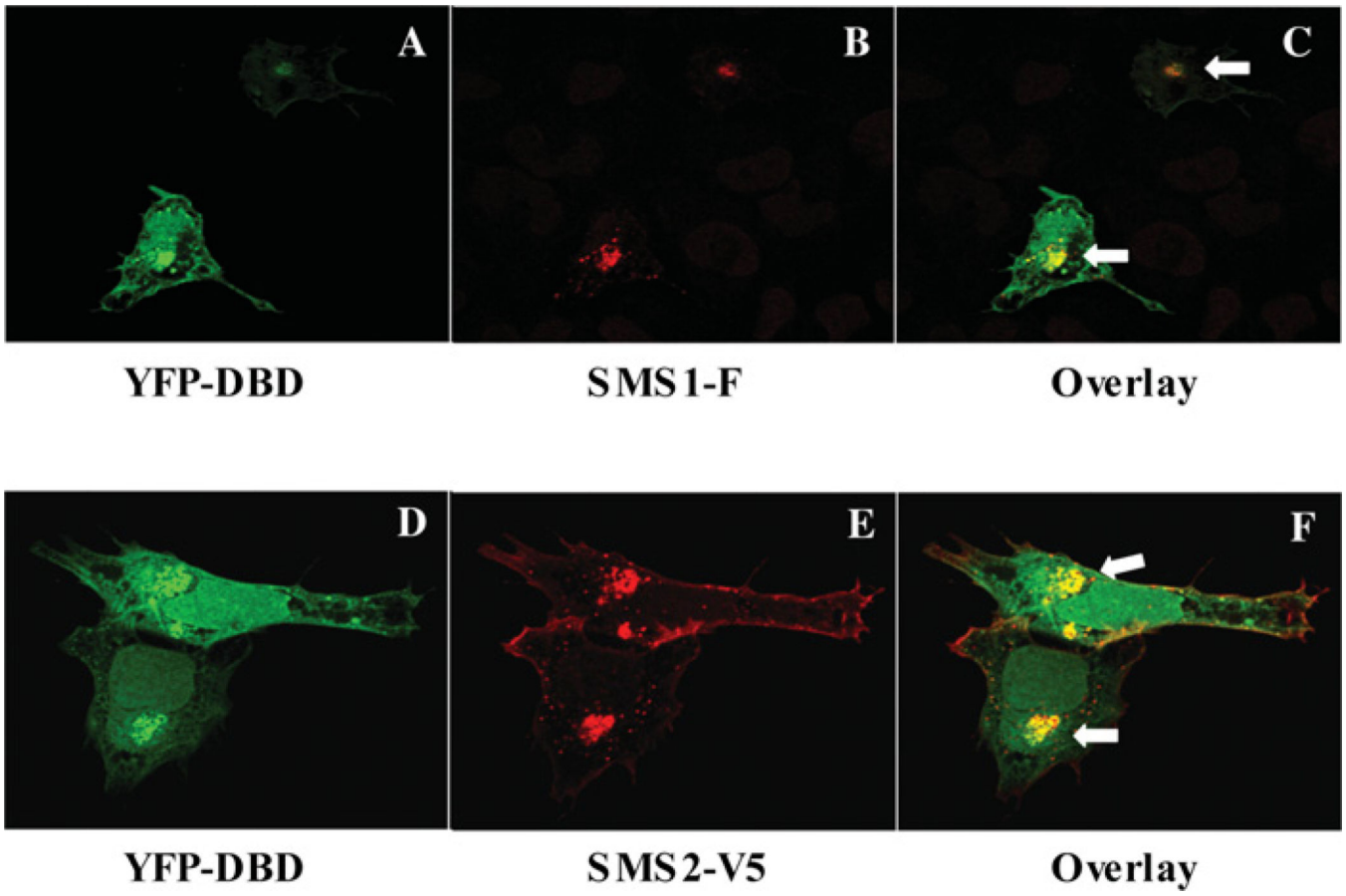

Figure 4. The site of DAG formation from metabolism of short-chain ceramide co-localizes with SMSs at the Golgi

HeLa cells were co-transfected with YFP–DBD (green) and with either pcDNA3.1 carrying SMS1–FLAG (SMS 1-F; **A–C**) or SMS2-V5 (**D–F**) for 22 h. Cells were then treated with 3 μM D-e-C_6-ceramide for 1 h, fixed and processed for immunofluorescence using monoclonal anti-FLAG (**A–C**) or anti-V5 (**D–F**) antibodies and stained with secondary Alexa Fluor® 633-conjugated anti-mouse antibodies (red). Samples were analysed by confocal microscopy. Confocal images were captured and processed using the LSM 510 META. Images are representative of at least two independent experiments. Arrows indicate sites of co-localization.

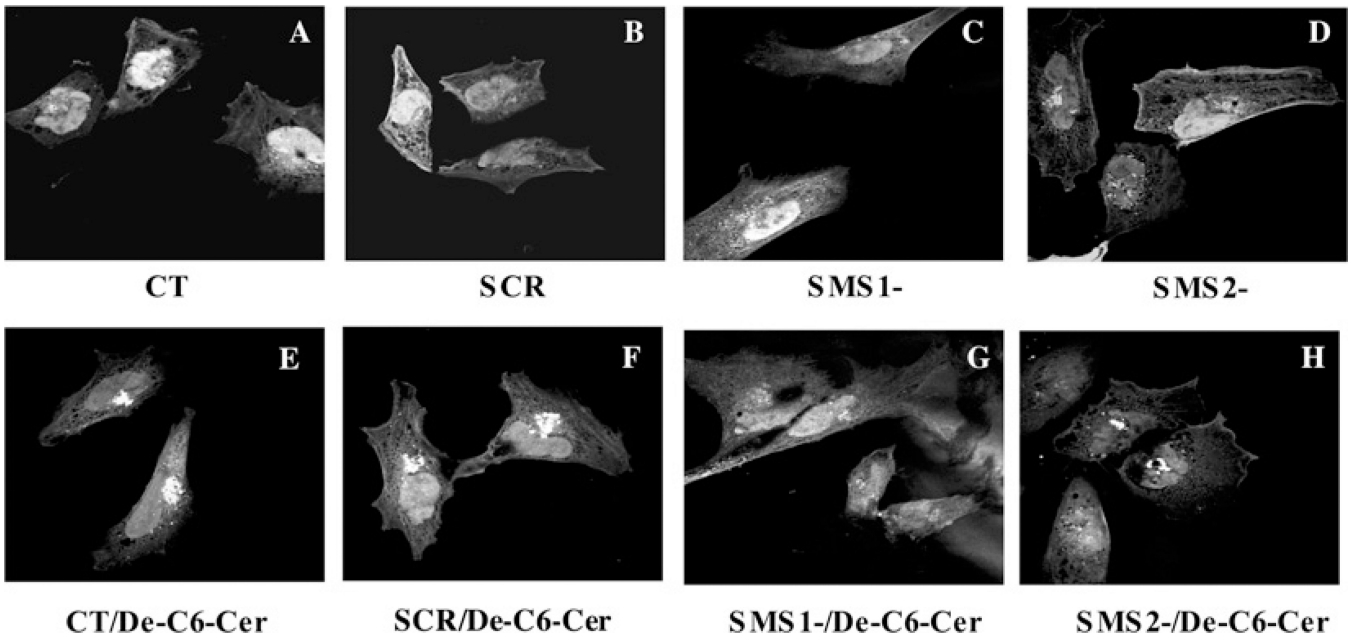

Figure 5. SMS1 and SMS2 are responsible for production of DAG from the metabolism of short-chain ceramide

HeLa cells were treated with Oligofectamine™ (CT; **A** and **E**), 10 nM SCR (**B** and **F**), siRNA targeting *SMS1* (SMS1−; **C** and **G**) or *SMS2* (SMS2−; **D** and **H**) for 48 h. Cells were then transfected with 1 μg of YFP–DBD for 22 h. Cells were then left untreated (**A–D**) or treated with 3 μM of D-e-C_6-ceramide (D-e-C6-Cer) for 1 h (**E–H**) and then fixed and analysed by confocal microscopy. Confocal images were captured and processed using the LSM 510 META. The images are representative of at least three independent experiments.

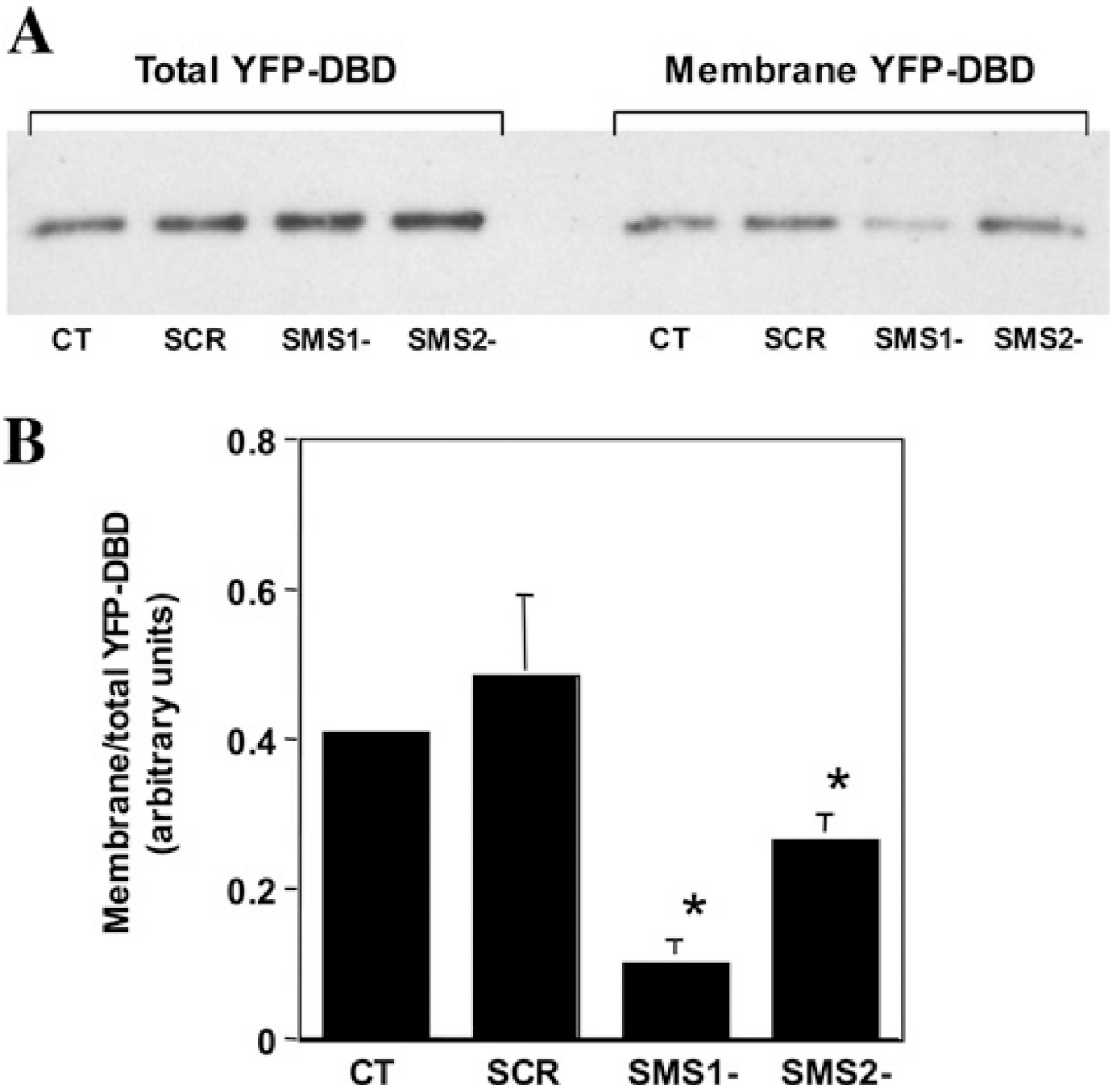

Figure 6. SMS1 and SMS2 modulate the levels of YFP–DBD in the membrane fraction

(**A**) The levels of total YFP–DBD and its membrane-associated fraction after down-regulation of SMS1 (SMS1−) or SMS2 (SMS2−) and C_6-ceramide treatment were determined by Western blotting analysis. (**B**) Quantification of the ratio between the levels of YFP–DBD associated with the membrane fraction and the total transfected YFP–DBD present in each sample is reported. The Labwork software was used for quantification of the intensity of the bands on the gel. (**A**) shows a representative experiment. Results from quantification shown in (**B**) are the means of three independent measurements. Error bars represent S.D. and $*P < 0.05$ compared with control (CT).

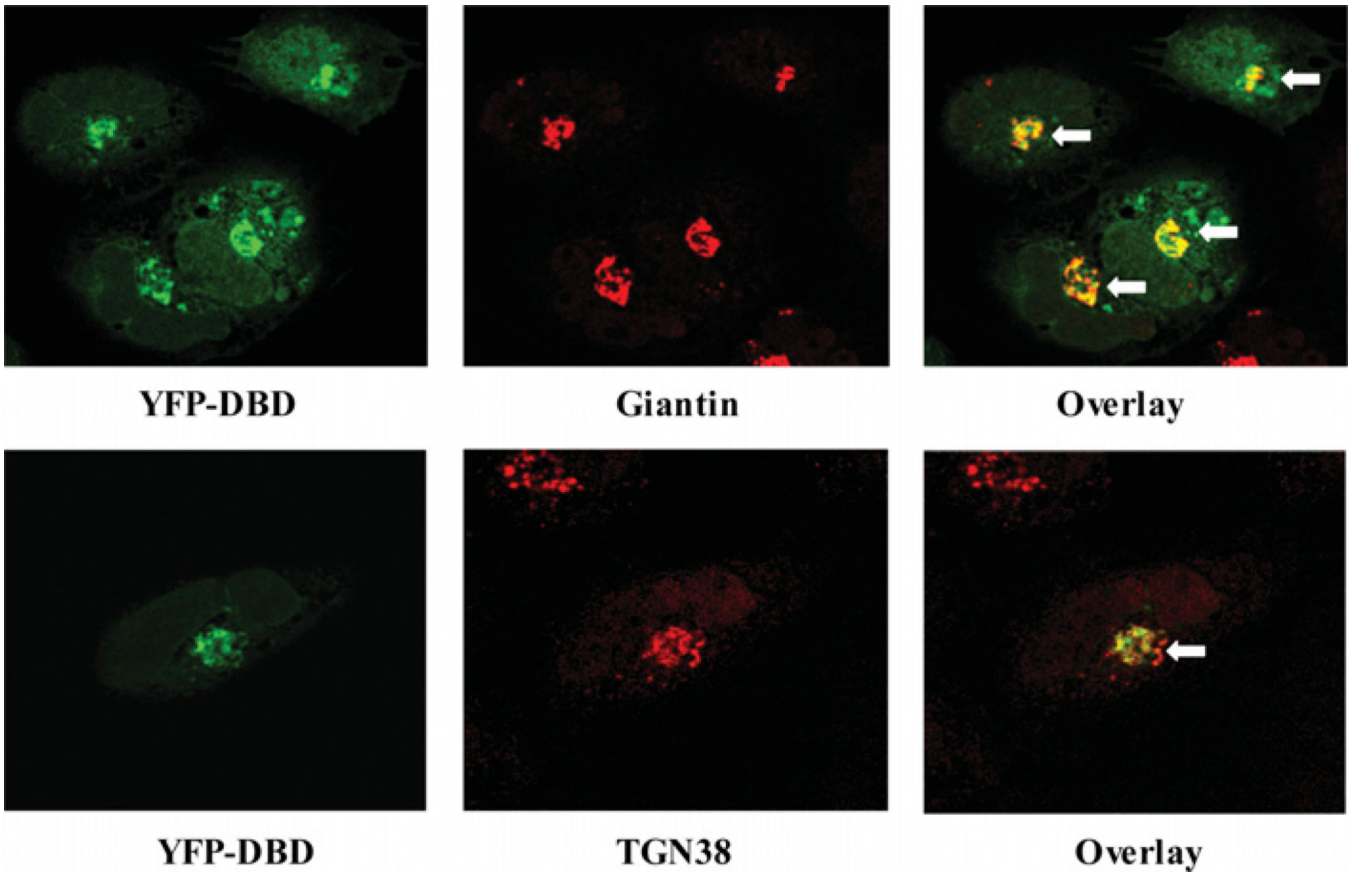

Figure 7. In SV40-transformed WI38 cells, stimulation of SM synthesis induces localization of the YFP–DBD to the Golgi

SV40-transformed WI38 cells transiently overexpressing YFP–DBD were treated with 3 μM C_6-ceramide for 1 h. After fixation, indirect immunofluorescence was performed using anti-giantin or anti-TGN38 antibodies. The co-localization of YFP–DBD with both proteins indicates the Golgi localization of YFP–DBD. Confocal images were captured and processed using the LSM 510 META.

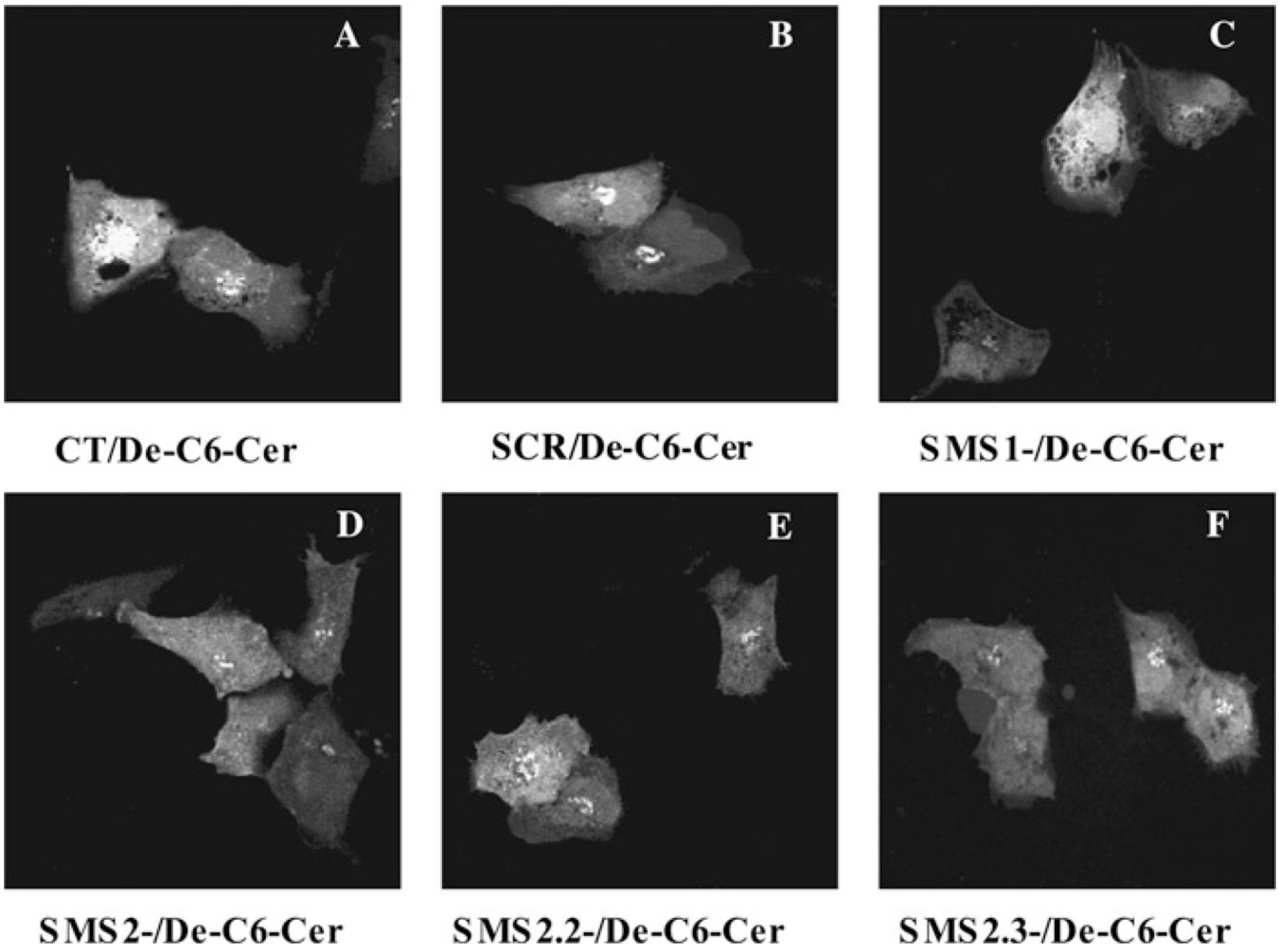

Figure 8. SMS1 and SMS2 are responsible for production of DAG from the metabolism of short-chain ceramide in SV40-transformed WI38 fibroblast

SV40-transformed WI38 fibroblasts were treated with Oligofectamine™ (CT) (**A**), 10 nM SCR (**B**) or siRNA targeting *SMS1* (SMS1−) (**C**) or *SMS2* (SMS2−) (**D**) for 48 h. Cells were then transfected with 1 μg of YFP–DBD for 22 h. Cells were then treated with 3 μM D-e-C_6-ceramide (De-C_6-Cer) for 1 h and then fixed and analysed by confocal microscopy. Confocal images were captured and processed using the LSM 510 META. (**E**) and (**F**) Cells were treated with 5 nM of two additional siRNA sequences targeting SMS2 [5 nM of SMS2.2− or SMS2.3− were found to cause maximal down-regulation of SMS2 as determined by RT–PCR (reverse transcription–PCR)]. The images are representative of two independent experiments.

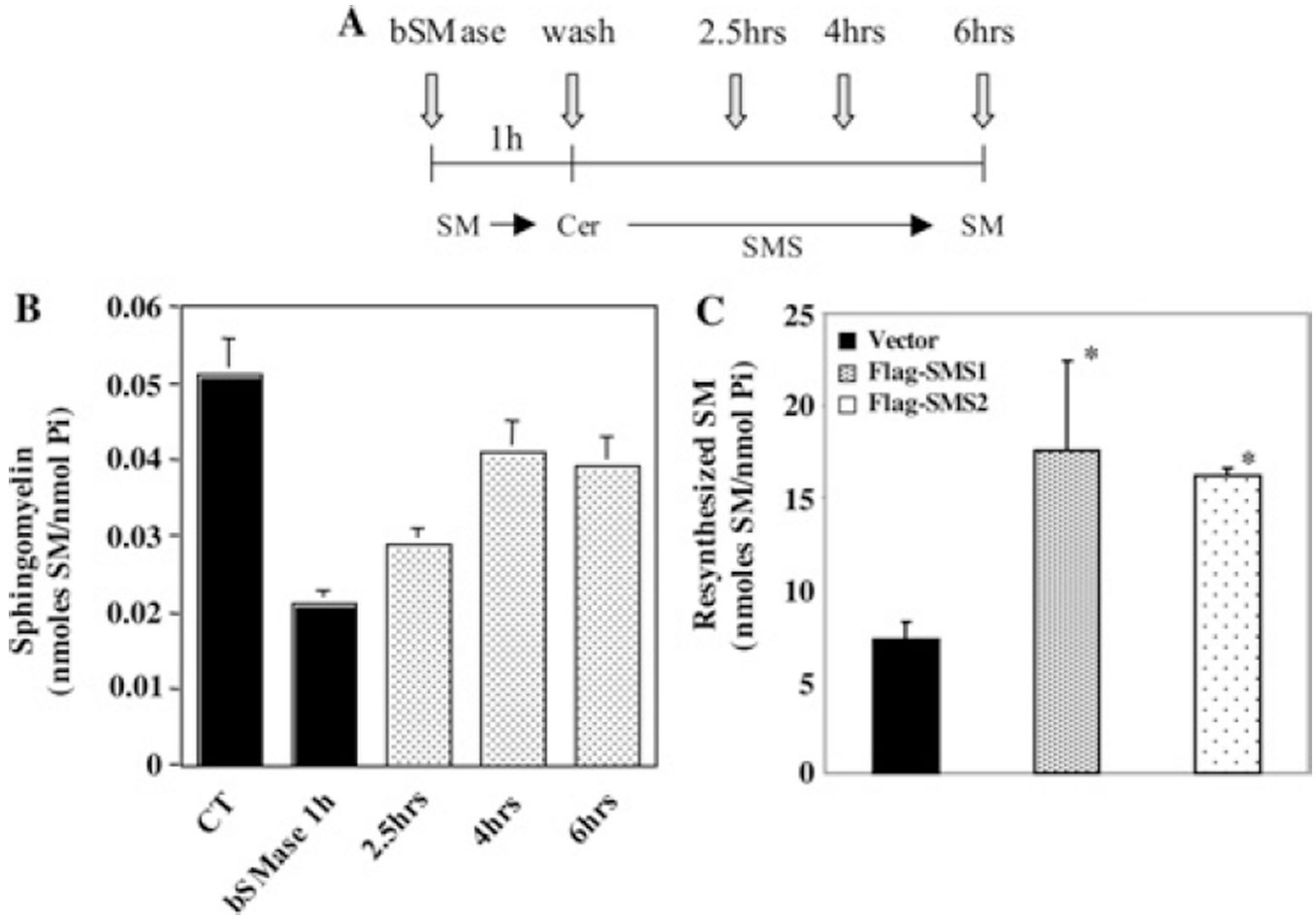

Figure 9. Both SMS1 and SMS2 regulate SM synthesis from ceramide produced at the plasma membrane

(**A**) A schematic diagram of the experimental conditions used in (**B**) and (**C**). After being exposed to 1 h treatment with 50 mU/ml bSMase, cells were washed thoroughly and incubated for up to 6 h in the absence of bSMase. Cells were collected at the indicated time points and lipid analysis was performed for non-radioactive SM measurements as described in the Experimental section. For (**C**), after overexpression of FLAG–SMS1 or FLAG–SMS2 for 18 h, HeLa cells were treated with 50 mU/ml of bSMase for 1 h followed by 2.5 h of incubation in the absence of bSMase; cells were then rinsed, collected in ice-cold PBS, and lipid analysis was performed for non-radioactive SM measurements as described in the Experimental section. The values are representative of at least 3 independent experiments, and error bars represent S.D. and $*P < 0.05$ compared with vector control.

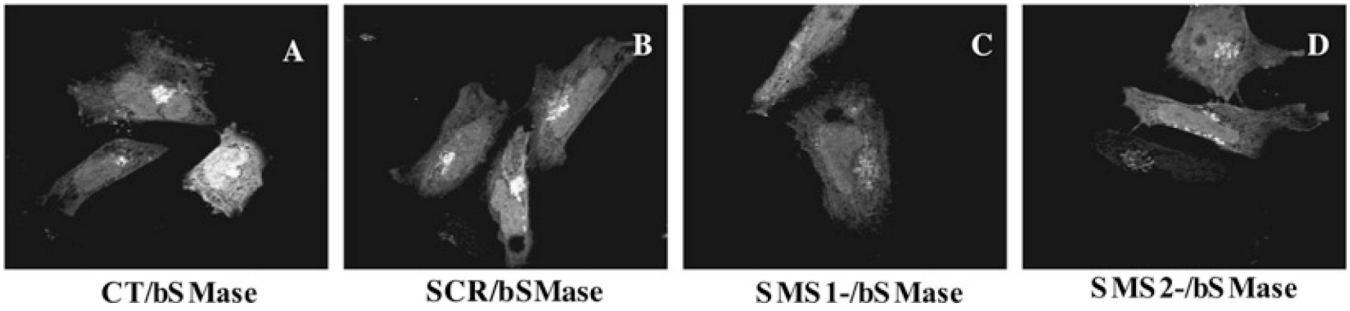

Figure 10. SMS1 and SMS2 are responsible for production of DAG from the metabolism of ceramide generated at the plasma membrane

HeLa cells were treated with Oligofectamine™ (CT) (**A**), 10 nM SCR (**B**) or siRNA targeting *SMS1* (SMS1−) (**C**) or *SMS2* (SMS2−) (**D**) for 48 h. Cells were then transfected with 1 μg of YFP–DBD for 22 h. Cells were then treated with bSMase as indicated in Figure 9. After the removal of bSMase, cells were incubated for 3 h, and then fixed and analysed by confocal microscopy. Confocal images were captured and processed using the LSM 510 META. The images are representative of at least three independent experiments.

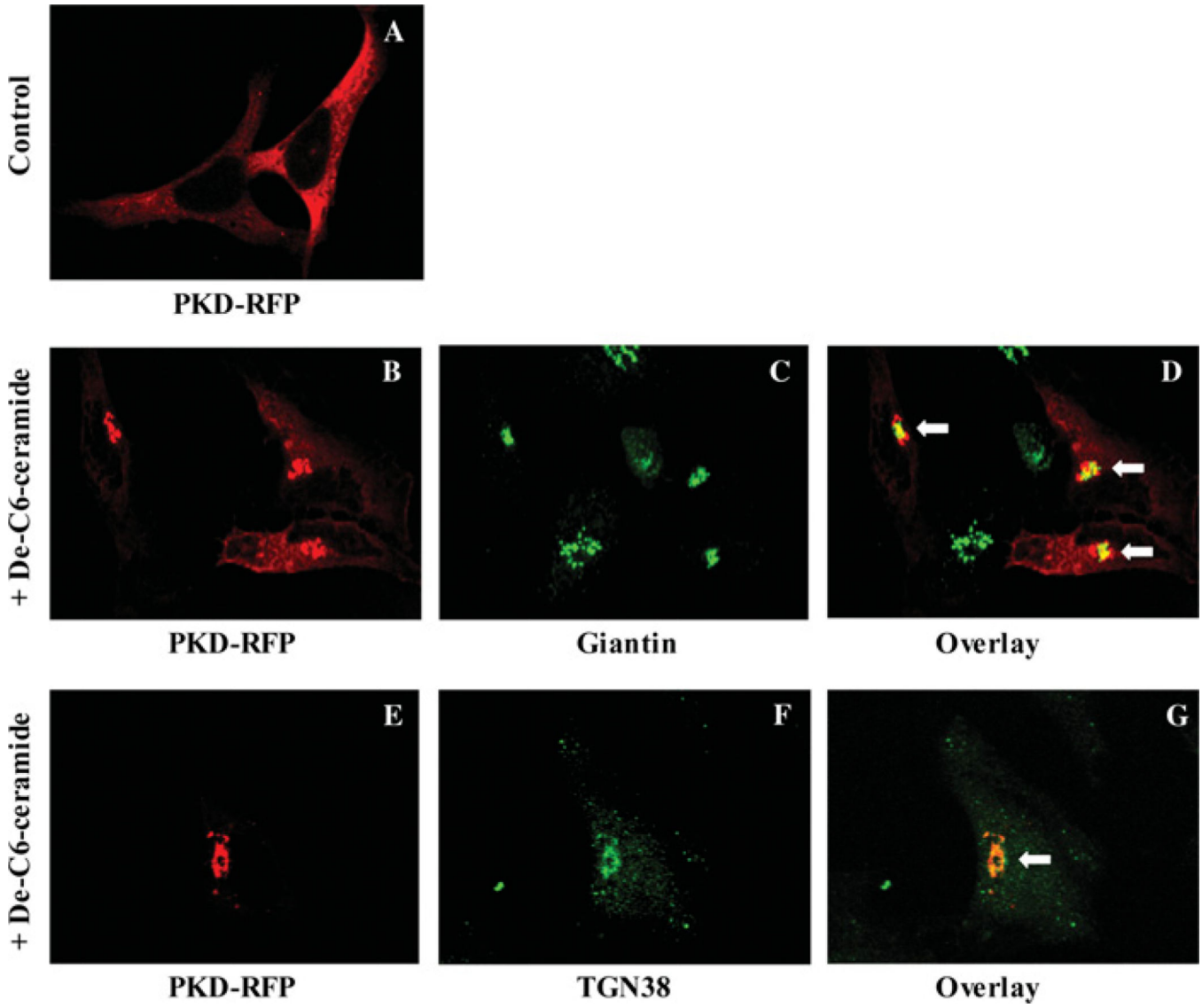

Figure 11. Stimulation of SM synthesis induces localization of PKD to the Golgi

HeLa cells transiently overexpressing PKD–RFP (red) were either left untreated (**A**) or treated with 3 μM C_6-ceramide for 1 h and then fixed (**B–G**). For (**B–G**), indirect immunofluorescence was performed using anti-giantin (**C** and **D**) or anti-TGN38 (**F** and **G**) antibodies (green). The co-localization of PKD–RFP with giantin and TGN38 (arrows) indicates Golgi localization of PKD–RFP. Confocal images were captured and processed using the LSM 510 META. The images are representative of two independent experiments.

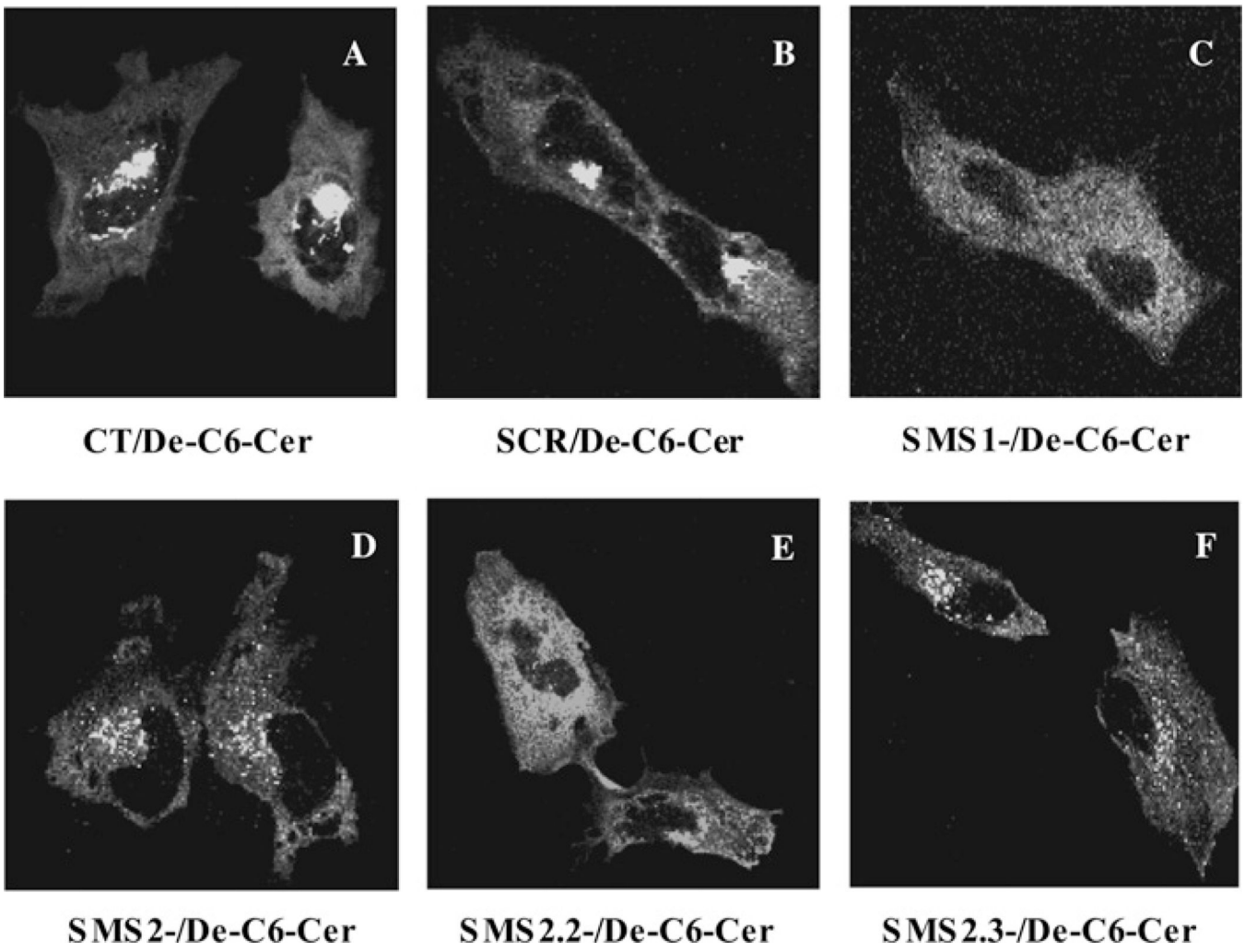

Figure 12. SMS1 and, to a lesser extent, SMS2 regulate localization of PKD to the Golgi in response to stimulation of SM synthesis

HeLa cells were treated with Oligofectamine™ (CT) (**A**), 10 nM SCR (**B**) or siRNA targeting *SMS1* (SMS1−) (**C**) or *SMS2* (SMS2−) (**D**) for 48 h. Cells were transfected with 1 μg of PKD–RFP for 22 h. Cells were then treated with 3 μM of D-e-C_6-ceramide (De-C_6-Cer) for 1 h and then fixed and analysed by confocal microscopy. Confocal images were captured and processed using the LSM 510 META. (**E** and **F**) Cells were treated with 5 nM of two additional siRNA sequences targeting *SMS2* (SMS2.2− or SMS2.3− respectively). The images are representative of three independent experiments.